Journal of Environmental Chemical Engineering 7 (2019) 102787

Contents lists available at ScienceDirect

Journal of Environmental Chemical Engineering

journal homepage: www.elsevier.com/locate/jece

# Adsorption of heavy metals from coal acid mine drainage by shrimp shell waste: Isotherm and continuous-flow studies

Dámaris Núñez-Gómez[a,*], Caroline Rodrigues[a], Flávio Rubens Lapolli[a], María Ángeles Lobo-Recio[a,b]

[a] Department of Environmental Engineering, Federal University of Santa Catarina (UFSC), Florianópolis, SC, Brazil
[b] Department of Energy and Sustainability, Federal University of Santa Catarina (UFSC), Araranguá, SC, Brazil

ARTICLE INFO

*Keywords:*
Acid mine drainage (AMD)
Sorption
Waste biomaterial
Heavy metals
Isotherm
Fixed bed column

ABSTRACT

The main characteristics of coal acid mine drainage (AMD) are low pH and high concentrations of sulfate and different metallic ions. The objective of this research was to study the sorption equilibrium of the removal of metal ions and acids present in coal AMD using shrimp shell *in natura* (SS) as a biomaterial as well as the behavior of the continuous-flow removal process. The isotherms assays were carried out with synthetic solutions and natural AMD aiming to identify significant differences on metals ions removal by SS. Five isotherm models were studied. $R^2$ values and error statistical functions studies showed that the Freundlich isotherm model was the most appropriate for fitting the experimental data with both synthetic solutions and natural AMD, indicating a metallic removal via a physisorption mechanism. The removal of metal ions in continuous descendent flow was up to 90% Fe and 88% Mn, and the pH increased from 3.49 to 6.77. The adsorption capacities of Fe and Mn resulted in 17.43 and 3.87 mg $g^{-1}$ SS, respectively. Computing chemical modelling (Visual MINTEQ® software) indicated the sorption was a predominant mechanism on AMD remediation with SS, but with high pH-dependence. This study confirms the suitability of the proposed treatment and provides valuable information for designing a low-cost remediation process for AMD.

## 1. Introduction

In the last century, mining practices have generated serious environmental changes, making it virtually impossible to maintain natural ecosystems, causing environmental problems around the world [1–5]. Such is the case in the study area of Santa Catarina, Brazil [6–10]. Extraction and processing methods, and the use of coal generate highly toxic effluents and acid mine drainage (AMD) with low pH values (pH < 4.0) and significant high metal ion concentrations (Fe, Al, Mn, Cu, Zn, Pb and others) and sulphides. These effluents contaminate the superficial and natural ground waters, causing environmental problems that can damage ecosystems and human health [11].

Generally, the pyrite ($FeS_2$) contained in coal is described as responsible for acid generation and metal dissolution. When pyrite is exposed to oxygen and water, it is oxidized, resulting in the release of hydrogen ions, sulfate ions, and soluble metal cations. This oxidation process occurs at a slow rate, and the environment is able to buffer the acid generated. Mining increases the exposed surface area of these sulfur-bearing rocks, allowing for excess acid generation beyond the natural buffering capabilities of the environment [12–14].

Acid generation and metal dissolution are the primary problems associated with pollution from mining activities. The chemistry of these processes appears fairly straightforward, but it becomes complicated quickly as geochemistry and physical characteristics can vary greatly from site to site [15].

In general, traditional treatment of AMD involves chemical processes and requires the three following processes: the addition of a neutralizing agent, decreasing the $SO_4^{2-}$ concentration, and the removal of other dissolved and/or particulate contaminants (metal and/or metalloid ions) [16]. Due to limited water resources and the very high cost of traditional treatment, alternative treatments and innovative technologies have been investigated to offer a viable solution to the environmental threats created by closed mines. These treatments include the use of natural biomaterials such as chitin. Crustacean shells (such as shrimp) are composed of a complex solid matrix of chitin (poly-*N*-acetylglucosamine), protein, and $CaCO_3$, providing alkalinity, and are capable of removing dissolved metals due to their sorbent characteristics [17,18].

The hydric resources of the coal basin of Santa Catarina, Brazil, are strongly impacted by coal AMD, and its water cannot be used [19]. This

* Corresponding author.
*E-mail address:* damaris_ng@hotmail.com (D. Núñez-Gómez).

https://doi.org/10.1016/j.jece.2018.11.032
Received 24 August 2018; Received in revised form 14 October 2018; Accepted 16 November 2018
Available online 17 November 2018
2213-3437/ 

research has the final objective of transforming coal AMD to water adequate for non-potable reuse, considering the preservation of the limited water sources of high quality for potable use. Thus, shrimp shells were used as an AMD treatment agent due to their low cost (it is a very abundant reject in Santa Catarina) and high chitin content. Shrimp shell is also used as a metal ion biosorbent, and calcium carbonate is used as an acid neutralizing agent. Since it is a waste-product of the seafood industry, provides the following twofold benefits: (a) it can reduce the concerns related to waste material disposal and degradation and (b) it can reduce the overall cost of remediation technologies. Preliminary studies demonstrated that shrimp shells are a better AMD treatment agent than processed chitin [17].

Thus, in continuity with kinetic studies [16], in this paper, experimental tests were conducted to determine the sorption equilibrium of Fe and Mn removal onto shrimp shell waste employing different isotherm models. To determine the adsorption characteristics for practical application, metallic ion removal studies in a packed bed column in continuous-flow conditions were also made.

## 2. Materials and methods

### 2.1. Biomaterial

Our previous studies explored the feasibility of utilizing shrimp shells as an acidic and metal ions removal agent for AMD remediation [16,17,20,21]. Shrimp shells (without the head) were processed according to own methodology, where was meticulously washed with tap water to eliminate the remains of organic matter; subsequently, the shrimp shells were dried in an oven for 72 h (48 h at 100 °C and 24 h at 50 °C). Once dry, the shrimp shells were pulverized in a blender and sieved to promote a greater homogeneity and contact surface area [16,17,20,21]. Prepared shrimp shells will be referred to as "SS" in this paper.

### 2.2. Equilibrium isotherms

Adsorption equilibrium experiments were carried out by varying the initial concentrations of Fe ions (10, 40, 80 and 120 mg $L^{-1}$) and Mn ions (4, 6, 8 and 12 mg $L^{-1}$) in separated synthetic solutions of $FeSO_4.7H_2O$ and $MnSO_4.H_2O$, respectively. For all the tests, 100 mL of the solutions were placed in non-sterile, polypropylene Erlenmeyer flasks with a 250 mL total capacity. The required amount of the adsorbent (11.46 g $L^{-1}$ of SS) was added and the flasks were capped with plastic wrap to prevent the entry of environmental dirt and/or water from the thermostatic bath. The solutions were agitated for 24 h at 136 rpm (Dubnoff 252) at constant temperature (25 ± 2 °C). At the end of the given contact time, the mixture was rapidly filtered. The SS amount and agitation speed were previously determined using factorial experimental planning [20,21]. The samples were filtered (0.22 µm cellulose acetate membrane), and the residual metallic ion content was determined by atomic absorption spectroscopy (AAS) following USEPA Method 3005 A [22]. A parallel control experiment without SS was also carried out. The pH of the solution was measured during all processes.

In addition, isotherm tests with natural AMD were carried out in order to verify the interference/synergies with other AMD pollutants species as well as their coexistence in the same AMD solution and corresponding dilutions. AMD samples were collected from a 33-year-old inactive coal mine in southern Santa Catarina. The samples were collected, transported and maintained by following the specific methodology of the Standard Methods for the Examination of Water and Wastewater [23]. Metal ion concentrations were determined by atomic absorption spectroscopy (AAS) following USEPA Method 3005 A [22]. Different AMD dilutions (0%, 25%, 50%, 75% and 90%) were performed for adsorption equilibrium experiments. The initial characterization of the AMD dilutions used in the isotherm assays, as well as the nomenclature for each tested condition, are showed in Table 1. For all the tests, the initial pH (2.79) was constant. The other experimental conditions (SS content, agitation, contact time, etc.) were the same as those for the synthetic solutions.

**Table 1**
Initial characterization of Fe and Mn ions concentration for natural AMD dilutions used in isothermal tests and their respective nomenclature. Initial pH was 2.79. Where $\bar{\chi}$ is the average and σ is the standard deviation.

| Dilution | Nomenclature | [Fe] (mg $L^{-1}$) ($\bar{\chi} \pm \sigma$) | [Mn] (mg $L^{-1}$) ($\bar{\chi} \pm \sigma$) |
|---|---|---|---|
| 0% | $AMD_0$ | 74.22 ± 0.03 | 4.68 ± 0.08 |
| 25% | $AMD_{25}$ | 62.36 ± 0.05 | 3.82 ± 0.02 |
| 50% | $AMD_{50}$ | 50.54 ± 0.02 | 2.64 ± 0.04 |
| 75% | $AMD_{75}$ | 15.34 ± 0.03 | 1.38 ± 0.02 |
| 90% | $AMD_{90}$ | 5.23 ± 0.06 | 1.02 ± 0.04 |

The amounts of metal ions adsorbed by the adsorbent were taken as the difference between the initial and final ion solution concentrations. The amounts of adsorbed metal ions at equilibrium, $q_e$ (mg $g^{-1}$), were calculated by Eq. (1) [24]:

$$q_e = \frac{(C_0 - C_e)v}{w} \quad (1)$$

where $C_o$ and $C_e$ (mg $L^{-1}$) are the initial and equilibrium concentrations of the metal ions in water, respectively, $v$ is the volume of the solution (L), and $w$ is the mass of dry adsorbent used (g).

Analysis of equilibrium data is important for the industrial application of biosorption, since it gives comparison information among different biomaterials under various operating procedures. Adsorption isotherm models are widely employed to examine the relationship between sorbed ($q_e$) and aqueous concentrations ($C_e$). Although a range of isotherm models are available to study the equilibrium data, only the Langmuir, Freundlich, Temkin, Dubinin-Radushkevich and Sips isotherms models were used to study the sorption of metal ions onto SS.

### 2.3. Error functions study

In order to investigate the mechanism of sorption and the potential controlling steps, several error calculation functions have been used (Table 2). The parameters were determined using Solver add-in of Microsoft® Excel 2016.

### 2.4. Column studies on AMD remediation

In addition, continuous-flow sorption experiments were conducted in a glass column at room temperature (23 ± 4 °C) (Fig. 1). The column was designed with an internal diameter of 1.2 cm and a length of 80 cm. The bed height was kept at 34.5 cm. The experimental conditions are summarized in Table 3. A peristaltic pump (mark Milan BP600/1) was used to feed the AMD into the column.

**Table 2**
Statistical functions used to estimate the error deviations between experimental and theoretical predicted isotherm model values for Mn in a synthetic solution.

| Error functions | Equation | Where: |
|---|---|---|
| Average relative error | $ARE = \frac{1}{N}\sum\left(\frac{q_c - q_e}{q_e}\right)100$ | N: number of experimental data points; $q_c$: theorical calculated adsorption capacity at equilibrium (mg $g^{-1}$); $q_e$: experimental adsorption capacity at equilibrium (mg $g^{-1}$) P: number of parameters in each isotherm model |
| Sum of the squares of the errors | $ERRSQ = \sum (q_c - q_e)^2$ | |
| Marquardt's percentage standard deviation | $MPSD = \sqrt{\frac{\sum\left(\frac{(q_e - q_c)}{q_e}\right)^2}{N-P}}$ | |
| Hybrid fractional error function | $HYBRID = \frac{1}{N-P}\sum\left(\frac{q_e - q_c}{q_e}\right)100$ | |

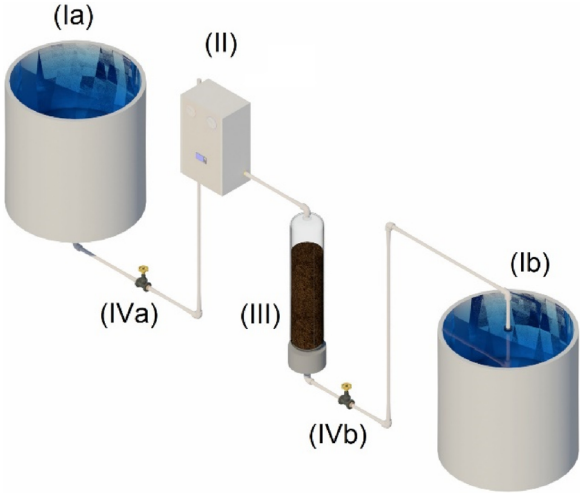


**Fig. 1.** Column experiment setup, where (Ia) and (Ib) are the initial and final reservoir, respectively; (II) peristaltic pump; (III) sorption column; (IVa) and (IVb) valves.

**Table 3**
Conditions for adsorption experiments in SS fixed bed column.

| | Parameters |
|---|---|
| Average flow (Q) | 7.8 $cm^3 min^{-1}$ |
| Hydraulic Retention Time (HRT) | 5 min |
| SS Volume | 39 $cm^3$ |
| SS Mass | 47.22 g |

During the adsorption process, effluent samples were collected at predetermined times. The column was operated for 900 min, in which the SS was saturated. The metallic ion concentrations were determined by AAS [22]. The pH of the samples was also measured (ThermoFisher Orion 3Stars pH meter). The breakthrough curves were drawn as a function of the AMD volume passed through the column. Control experiments without sorbent but maintaining the same flux were carried out to ascertain that the removal was by the sorbent and not by other mechanisms.

The total quantity of metal ion mass biosorbed in the column ($M_{ad}$) was calculated from the area above the breakthrough curve (outlet metal ion concentration vs time) multiplied by the flow rate. Dividing the metal ion mass ($M_{ad}$) by the biosorbent mass (M) leads to determination of the uptake capacity (Q) of the biomass. The total amount of metal ions sent to the column was calculated from the following equation [25]:

$$M_{total} = \frac{C_0 F t_e}{1000} \quad (2)$$

where $C_0$ is the inlet metal ion concentration (mg $L^{-1}$), F the volumetric flow rate (mL $h^{-1}$) and $t_e$ is the exhaustion time (h). Total metal ion removal (%) can be calculated from the ratio of metal ion mass adsorbed ($M_{ad}$) to the total amount of metal ions sent to the column ($M_{total}$) as follows [25]:

$$Total \quad metal \quad removal\ (\%) = \frac{M_{ad}}{M_{total}} 100 \quad (3)$$

### 2.5. Acid mine drainage (AMD)

For column studies, AMD from a closed mine within the coalfield area of Santa Catarina was collected. Samples were taken in non-sterile polypropylene containers and capped with minimal headspace. All the sample materials and containers were prewashed with detergents and acid and deionized water rinsed. The samples were transported and stored in a refrigerator at constant temperature of 4 °C [23] and characterized on the same day of collection for determination of the pH (pH meter ThermoFisher, Scientiphic Orion 3Stars) and metallic and metalloid species (ICP-MS, Perkin Elmer, Nexlon 300D).

### 2.6. Analytical methods

The concentration of the Fe and Mn ions were analyzed using AAS according to the procedure described in the USEPA Method (3005 A) [22]. Liquid samples were filtered through a 0.22 µm membrane filter (Sartorius Company) to remove solids and acidified with concentrated $HNO_3$ solution, to avoid precipitation of metals due to changes in pH [22]. A digital pH meter was used to monitor solution pH during the tests. Although previous tests [17,20,21] showed that, under these experimental conditions, SS is not an effective agent to eliminate sulfate, it was monitored by ion chromatography (Dionex ICS – 1000) during all experiments.

### 2.7. Visual MINTEQ modeling

The model of Visual MINTEQ [26,27] was commonly applied to describe heavy metal in soil, wastewater, and solid waste. A visual MINTEQ model was first used in geochemical study, and then it was gradually introduced in the research of environmental science and engineering. It can be used to calculate various chemical equilibrium processes including acid-base balance, dissolution-precipitation balance, redox balance, and adsorption balance. The software contains powerful equilibrium constants database, which can be modified.

In our case, the model was applied to simulate and predict the chemical equilibrium for the calculation of AMD metallic speciation to identify the principal species responsible for remediation (precipitates and/or adsorbed ions). AMD composite, before and after continuous-flow treatment with SS, was run with Visual MINTEQ 3.1 for predicting pH dependent metal speciation processes.

## 3. Results and discussion

### 3.1. Adsorption isotherm models

Adsorption isotherm models describe the distribution of the adsorbate species between liquid and adsorbent through plotted graphs based on a set of assumptions and related to the heterogeneity or homogeneity of adsorbents, the type of coverage, and the possibility of interaction between the adsorbates [28].

In this study, two different isothermal tests were performed. The first test, according to the traditional view, was carried out with a synthetic solution for each interest metal ion (Fe and Mn) (Fig. 2) in order to study the specific adsorption, avoiding competition for the active sites of the adsorbent by other species. For all the tests, an increase of the pH caused by the addition of SS to the synthetic solutions was observed. In both cases, for Fe and Mn isothermal tests, the final pH, after 24 h of contact time, was above to neutrality (pH > 7) confirming the influence and suitability of SS as a neutralizing agent due, mainly, to the calcium carbonate content. High metal ions removals were evidenced (> 99% for Fe and > 75% for Mn). In the case of Mn, the removal could be attributed to the process of adsorption onto SS, since pH values for its hydroxides precipitation (between 9 and 10) were not reached (Fig. 2b).

The second isotherm test was performed with natural AMD (Fig. 3) to identify the real adsorption behavior with the coexistence of several other metallic ions. As with the synthetic solutions, the addition of SS to the AMD samples caused the pH increase between 2 and 4 net points. In the more dilute samples ($AMD_{75}$ and $AMD_{90}$) pH values higher than neutrality was reached. Predictably, the addition of higher SS contents could guarantee the effective neutralization in the more concentrated

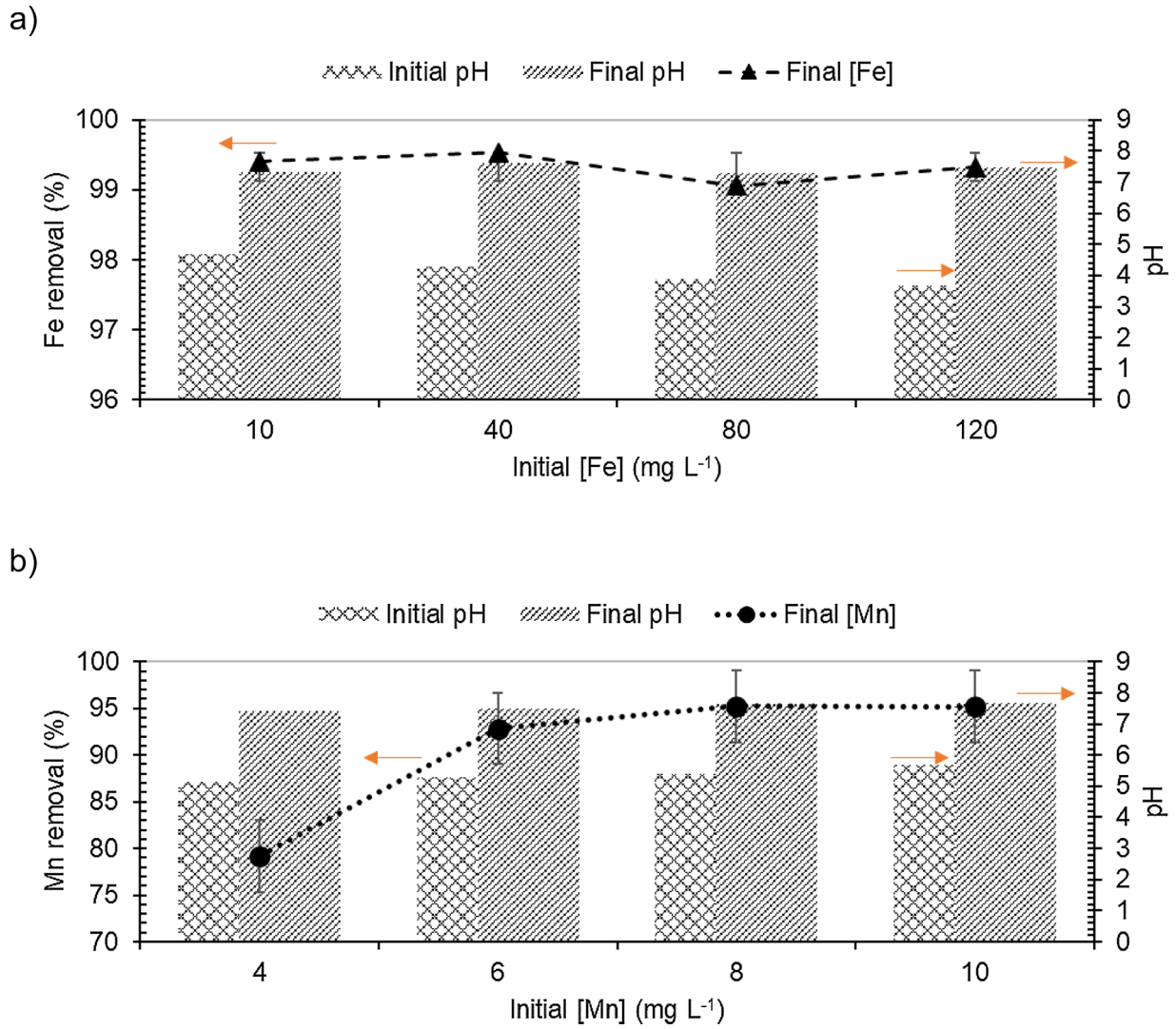


**Fig. 2.** Fe (a) and Mn (b) ions removal percentages and standard deviation from isothermal assays with synthetic solutions of $FeSO_4.7H_2O$ and $MnSO_4.H_2O$, respectively, and the pH variations in the tests versus the initial concentration (mg $L^{-1}$) of metal ion in the synthetic solutions; where the arrows indicate the respective ordinate axis of each parameter considered.

samples. Different behaviors were elucidated for metal ions removal as a function of the initial concentrations of the samples. While for the Fe ion removal lower initial concentrations showed higher percentual removals, for Mn ion the behavior was inverted. This can be explained by both the possible saturation of SS in high concentrations of Fe ions and the possible co-precipitation of the Mn ion in the presence of a high concentration of iron ions [29,30]. In natural AMD (without dilution - $AMD_0$), a 77–79% ion removal range was observed for both monitored metal ions. Mn ion removal percentage from natural AMD (Fig. 3) is lower than from synthetic solution (Fig. 2b), indicating a higher affinity of Fe ion with respect to the Mn ion for SS.

Based on the results, the inhibitory effect of the SS adsorption capacity in a multi-metal system when compared with mono-metal systems was confirmed. This effect could be due to the affinity and competition of ions for active sites on the adsorbent [31].

The most important multisite adsorption isotherm for

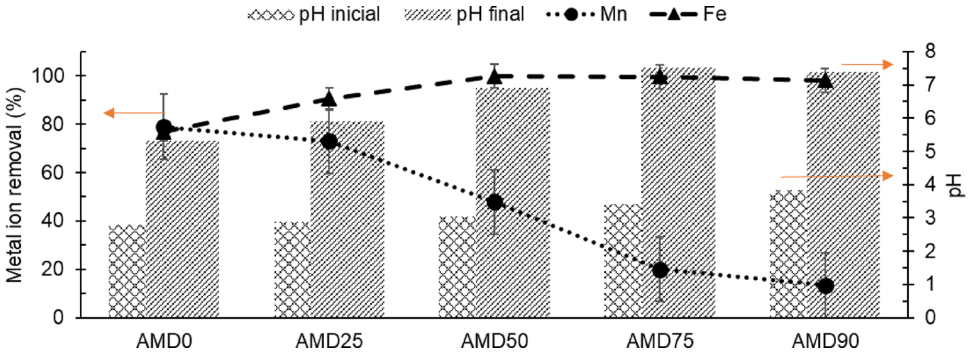


**Fig. 3.** Fe and Mn ions removal percentages and standard deviation from isothermal assays with natural acid mine drainage (AMD) and the pH variation in the tests versus different AMD dilutions; where $AMD_0$ and $AMD_{90}$ are, respectively, the non-diluted and the most diluted samples. The initial Fe and Mn ions concentrations in AMD samples were described in Table 1. The arrows indicate the respective ordinate axis of each parameter considered.

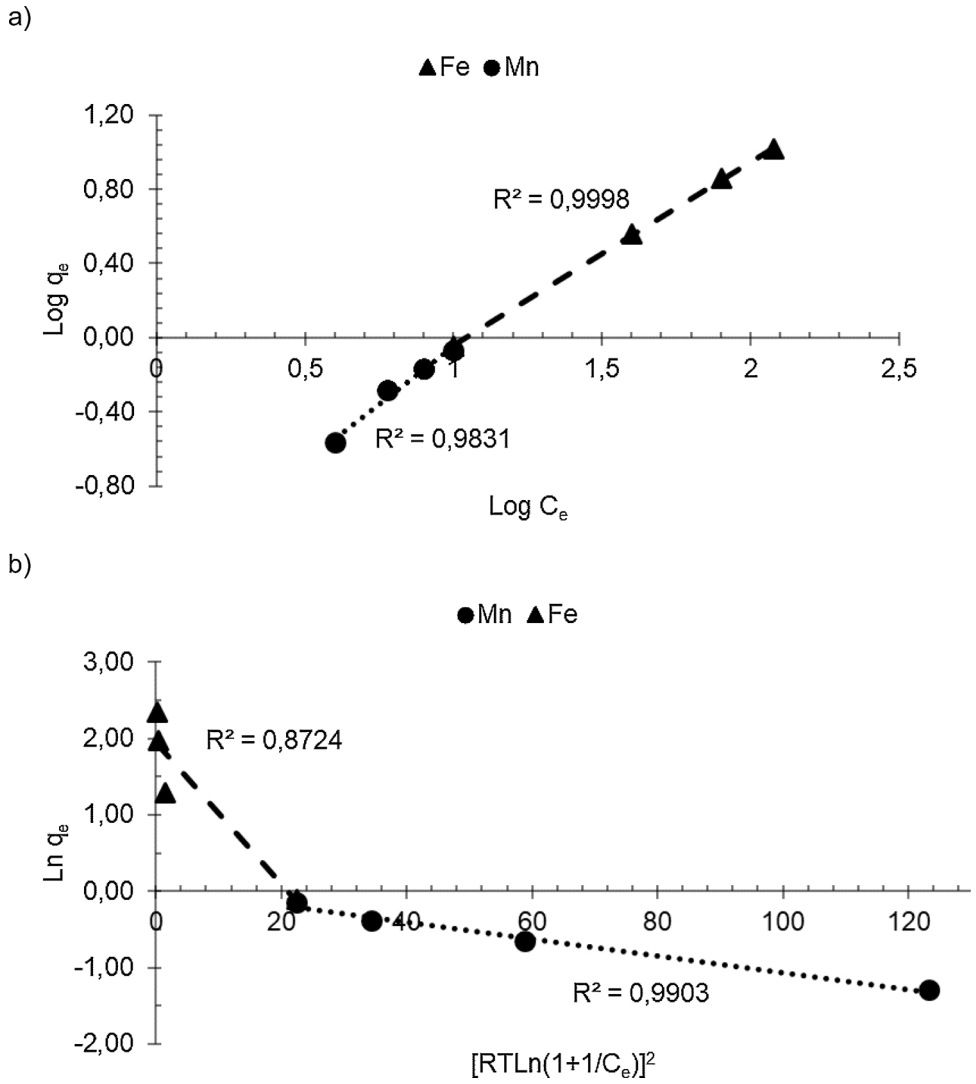


**Fig. 4.** The experimental adsorption data fit to (a) Freundlich and (b) Dubinin-Radushkevich isothermal models for Fe and Mn removal by SS in synthetic solutions.

heterogeneous surfaces is the Freundlich model. This empirical model can be applied to non-ideal sorption on heterogeneous surfaces as well as multilayer sorption. The linearized form of the Freundlich equation was used for analysis, and it is given as Eq. (4) [32].

$$\log q_e = \log K_F + \frac{1}{\eta}\log C_e \tag{4}$$

where $C_e$ is the equilibrium liquid phase ion concentration (mg $L^{-1}$), and $q_e$ is the equilibrium solid phase ion concentration (mg $g^{-1}$); $K_F$ is a Freundlich isotherm constant (mg $g^{-1}$), η the adsorption intensity. $K_F$ and $\eta^{-1}$ values can be calculated from intercept and slope of the linear plot between log $C_e$.

Data plots of log $q_e$ versus log $C_e$ (Fig. 4a) showed that the ion adsorption from synthetic solution onto SS follows the Freundlich isotherm model well with high correlation coefficients, $R^2$ = 0.9998 for Fe ions and $R^2$ = 0.9831 for Mn ions (Table 4). This indicates that the biosorption of the Fe and Mn onto SS fitted well for the Freundlich model. Large $K_F$ values indicate greater adsorption capacity. η is a function of the strength contrariwise of the used adsorbent material. A value of η > 1, as in the iron sorption (η = 1.01), indicates that the adsorption coefficient increases with increasing solution concentration. Otherwise, when the value of η < 1, (Mn η = 0.81), $K_F$ decreases with concentration [33]. Similar isotherm results were observed for Fe removal onto different adsorbents [34].

The Langmuir equation was chosen for the estimation of the maximum adsorption capacity corresponding to the complete monolayer coverage on the adsorbent surface [35]. The equation can be linearized into Eq. (5):

$$\frac{Ce}{q_e} = \frac{1}{q_m K_L} + \frac{Ce}{q_m} \tag{5}$$

where $q_m$ is the maximum amount of adsorption with complete monolayer coverage on the adsorbent surface (mg $g^{-1}$), and $K_L$ is the Langmuir constant related to the energy of adsorption (L $mg^{-1}$). The Langmuir constants $K_L$ and $q_m$ can be determined from the linear plot of $C_e/q_e$ versus $C_e$.

The essential characteristics of the Langmuir isotherm can be expressed in terms of $R_L$, and a dimensionless separation factor of equilibrium parameter is defined as Eq. (6) [36].

$$R_L = \frac{1}{1 + K_L C_0} \tag{6}$$

where $C_0$ (mg $L^{-1}$) is the initial adsorbate concentration. The value of $R_L$ indicates the shape of the isotherms to be unfavorable ($R_L > 1$), linear ($R_L = 1$), favorable ($0 < R_L < 1$) or irreversible ($R_L = 0$) [32].

The plot of ($C_e/q_e$ versus $C_e$) results of the Fe and Mn ion adsorption onto SS (Fig. 1a of Supplementary material) showed low $R^2$ value (< 0.6121) proved that the sorption data did not fit well to the

**Table 4**
Linear regression equations and isothermal constants for Freundlich and Dubinin-Radushkevich models for Fe and Mn adsorption onto SS in synthetic solutions.

| Isotherm model | Parameter | Fe | Mn |
|---|---|---|---|
| Freundlich | LR | $logq_e = 0.9903\frac{1}{\eta}$-1.0332 | $logq_e = 1.239\frac{1}{\eta}$-1.2881 |
| | $R^2$ | 0.9998 | 0.9831 |
| | $K_F$ (L mg$^{-1}$) | 0.093 | 0.059 |
| | $\eta$ | 1.01 | 0.81 |
| Dubinin-Radushkevich | LR | $ln\ q_e = -4E\text{-}05\left(1+\frac{1}{C_e}\right)- + 1.9416$ | $ln\ q_e = -4E\text{-}06\left(1+\frac{1}{C_e}\right)- + 0.0291$ |
| | $R^2$ | 0.8724 | 0.9903 |
| | $B_D$ | $8.07 \times 10^{-09}$ | $8.06 \times 10^{-10}$ |
| | $\mathscr{E}$ | 7872.13 | 24893.87 |
| | $K_D$ (L mg$^{-1}$) | 6.97 | 1.03 |

LR: Linear regression.

**Table 5**
Isothermal error deviation data related to the adsorption of Mn onto SS in synthetic solutions.

| | $R^2$ | ARE | ERSSQ | MPSD | HYBRID |
|---|---|---|---|---|---|
| Freundlich | 0.9831 | **31**.87768 | **2**.52027 | **11**.28674 | **5**.14503 |
| Dubinin-Radushkevich | **0.9903** | 78.26267 | 4.73788 | 17.26686 | 9.56871 |

Bold the lowest values of error functions. Where ARE is the average relative error; ERRSQ es the sum of squares of the errors; MPSD is the Marquardt's percentage standard deviation; and HYBRID is the hybrid fractional error function.

Langmuir Isotherm model. The equation, coefficient of correlation ($R^2$) generated and Langmuir constants are shown in Table 1 of Supplementary material.

However, the Temkin isotherm assumes that the heat of adsorption decreases linearly with the coverage due to adsorbent-adsorbate interaction [37]. The Temkin isotherm has generally been applied in the following linear form [38]:

$$q_e = B\ln K_T + B\ln C_e \tag{7}$$

$$B = \frac{RT}{b} \tag{8}$$

where $K_T$ (L mg$^{-1}$) is the Temkin isotherm constant, b ($J$ mol$^{-1}$) is a constant related to heat of sorption, R is the gas constant (8.314 J mol$^{-1}$ K$^{-1}$) and T is the absolute temperature (K). Based on the plot of $q_e$ versus ln $C_e$ (Fig. 1b of Supplementary material), a high $R^2$ (> 0.84) was determined, but minor when compared with other models like Freundlich for Fe ion and Dubinin-Radushkevich for Mn ion. The data are listed in Table 1 of Supplementary material.

The Dubinin-Radushkevich isotherm model was chosen to estimate the characteristic porosity of the biomass and the apparent adsorption energy. The linear form of the model is represented by the following equation:

$$\ln q_e = \ln K_D - 2B_D RT\ln\left(1+\frac{1}{C_e}\right) \tag{9}$$

where $B_D$ is related to the free energy of sorption per mole of the sorbate as it migrates to the surface of the biomass from an infinite distance in the solution, and $K_D$ is the Dubinin-Radushkevich isotherm constant related to the degree of sorbate sorption by the sorbent surface [39]. The apparent energy (E) of adsorption from the Dubinin-Radushkevich isotherm model can be computed using the relation given below [39].

$$E = \frac{1}{\sqrt{2B_D}} \tag{10}$$

The observed relationship of plot Ln $q_e$ versus $\left[RTln\left(1+\frac{1}{C_e}\right)^2\right]$ for Mn ion removal onto SS (Fig. 4b) was statistically significant as evidenced by the $R^2$ value close to the unit (0.9903). The information obtained with the Dubinin-Radushkevich's isotherm model permitted distinguish the type of adsorption that occurs between the adsorbent and the adsorbate; thus, in this case, and only for Mn ion, the adsorption energy determined that adsorption could be chemical [40]. In the other hand, for Fe ion, a smaller $R^2$ value (0.8724) when comparing with the Freundlich model (0.9998) indicated the not satisfactory correlation of this model. The calculated Dubinin-Radushkevich constants and mean free energy for adsorption are shown in Table 4.

Due to the close $R^2$ values, and in order to evaluate the fit of the Freundlich and Dubinin-Radushkevich isotherm equations to the experimental data, different statistical error functions were examined for the Mn-SS adsorption system in synthetic solution (Table 2). Among the two studied isothermal model, and according to Table 5, it seems that Freundlich model was the most suitable model to satisfactorily describe the Mn-SS adsorption phenomenon. Indeed, the lowest ARE, ERRSQ, MPSD and HYBRID values were found when modeling the isothermal data using Freundlich model, indicating sorption mechanisms via physisorption for Mn on SS. Such trend was previously proven by other researchers [41,42].

Finally, the Sips isotherm is derived from the limiting behavior of the Langmuir and Freundlich isotherms. The model is valid for localized adsorption without adsorbate-adsorbate interactions [28]. When the sorbent content approaches a low value, the Sips isotherm effectively reduces to the Freundlich isotherm; however, at high values, it predicts the Langmuir monolayer sorption characteristics. The Sips linear equation model is expressed as Eq. (11) [28].

$$\frac{1}{q_e} = \frac{1}{q_{max}K_S}\left(\frac{1}{C_e}\right)^{1/\eta} + \frac{1}{q_{max}} \tag{11}$$

where $K_S$ (mg L$^{-1}$) and $q_{max}$ (mg L$^{-1}$) are the Sips equilibrium constant and maximum adsorption capacity values obtained from the slope and the intercept of the plot (Fig. 1c of Supplementary material) [43]. The poor coefficient of determination values ($R^2$ = 0.6344 for Fe and $R^2$ = 0.3159 for Mn) suggests that it is not applicable to this model to represent the equilibrium sorption of Fe and Mn ions by SS (Table 1 of Supplementary material).

Comparing the correlation coefficients values obtained for each of the considered isotherms for synthetic solutions, the fitting degree follows the sequence: Freundlich > Dubinin-Radushkevich > Temkin > Langmuir > Sips. The Freundlich equation for Fe and Mn represented the best fits to the experimental data, with $R^2$ = 0.9998 and $R^2$ = 0.9831, respectively. These results are better than the results from the other isotherm models, indicating sorption mechanisms via physisorption. These results were confirmed by the statistical study of errors.

As mentioned above, adsorption equilibrium studies with natural AMD were performed. The adsorption results for Fe and Mn ions were different when compared to each other. While for Fe ions, the

**Table 6**
Linear regression equations and isothermal constants for Freundlich model for Fe and Mn adsorption onto SS in natural AMD.

| Isotherm model | Parameter | Fe | Mn |
|---|---|---|---|
| Freundlich | LR | $logq_e = 0.9415\frac{1}{\eta}$-0,9899 | $logq_e = 1.740\frac{1}{\eta}$-1.6627 |
| | $R^2$ | 0.9929 | 0.9663 |
| | $K_F$ (L mg$^{-1}$) | 0.102 | 0.0217 |
| | η | 1.062 | 0.575 |

LR: Linear regression.

Freundlich isothermal model remains the best model that describes the experimental data ($R^2$ = 0.9929), for Mn ions, the higher correlation coefficient changed from the Dubinin-Radushkevich model with synthetic solution to the Freundlich model as well ($R^2$ = 0.9663). This result indicates that the biosorptions of Fe and Mn onto SS in natural AMD were fit well by the Freundlich model. A large $K_F$ value indicates greater adsorption capacity. η is a function of the strength of the used adsorbent material. A value of η > 1, as in the iron sorption (η = 1.062), indicates that the adsorption coefficient increases with increasing solution concentration. Conversely, when the value of η < 1, (Mn η = 0.575), indicated that $K_F$ decreases with concentration [33]. The results are consistent with the description of SS with a heterogeneous surface. The weak $R^2$ values obtained for the Temkin, Dubinin-Radushkevich, Langmuir and Sips models indicate that the sorption data did not fit well with these. No bibliographic references were found for isothermal assays with AMD natural, so no comparison was possible. The linear regression equation and coefficient of determination ($R^2$) generated for Freundlich model are shown on Table 6. Complementary details from others isothermal models are presented in Table 2 of Supplementary material.

### 3.2. Characterization of AMD

AMD samples were characterized to define the target chemical species because of its high concentration and/or its dangerousness. $Fe_{total}$ and $Mn_{total}$ were the metal ions selected for monitoring during treatment with SS due to its high concentrations, well above the Brazilian legal limits (Table 7). The $SO_4^{2-}$ content was monitored during all experiments but did not change greatly after treatment (3630.8 mg L$^{-1}$), indicating that the SS under the conditions tested was not adequate for the removal of this contaminant, which is in line with previous research [16,17,20,21]. Complementary tests, under a nitrogen atmosphere, are being carried out to verify the potential of SS as a substrate for the development of sulphate-reducing bacteria (SRB) and thus promote the sulfate elimination.

**Table 7**
Initial characterization of AMD used in the tests.

| Variable | Unit | Value | CONAMA 430/2011[a] | CONAMA 357/2005[b] |
|---|---|---|---|---|
| pH | – | 3.49 | 5-9 | 6-9 |
| Sulfate | mg L$^{-1}$ | 3630.8 | NA | 250 |
| $Fe_{total}$ | mg L$^{-1}$ | 83.24 | 15.0 | 5.0 |
| $Mn_{total}$ | mg L$^{-1}$ | 5.94 | 1.0 | 0.5 |
| Al | mg L$^{-1}$ | 0.020 | NA | 0.2 |
| Nd | mg L$^{-1}$ | 27.67 × 10$^{-3}$ | NA | NA |
| Cd | mg L$^{-1}$ | 0.001 | 0.2 | 0.01 |
| Co | mg L$^{-1}$ | 0.078 | NA | 0.2 |
| Cu | mg L$^{-1}$ | 0.012 | 1.0 | 0.013 |
| Ni | mg L$^{-1}$ | 71.04 × 10$^{-3}$ | 2.0 | 0.025 |

NA: Not applied.
[a] Brazilian legal limits for effluent discharge [44].
[b] Brazilian legal limits for reuse water such as non-potable secondary use [45].

### 3.3. Column test

The results obtained from batch studies are important in providing information on the effectiveness of the sorbent system. However, this process is usually limited to the treatment of small effluent volumes under equilibrium conditions that do not give accurate scale-up data for industrial treatment systems where a continuous-flow regime is normally employed. Furthermore, uneven flow patterns throughout the column and the problems of regeneration cannot be meaningfully studied in a batch experiment. Therefore, it is necessary to carry out flow tests using columns to obtain design models, which would be applicable to commercial systems.

In this case, during the initial 60 min of continuous-flow operation, a rapid increase in pH was observed in the column effluent. Until 114 min, the pH remained relatively neutral and reached the maximum value of 6.79 (Fig. 5). A significant decrease in metal ion concentrations (90% Fe and 88% Mn) was observed during this initial stage of operation, possibly promoted by the coexistence of two simultaneous processes, adsorption onto SS and precipitation such as hydroxides (high pH values). After this, the removal was lowered until t = 762 min, when the SS was metal saturated. In these experimental conditions, the continuous-flow experiment showed that the Brazilian standard parameters for reusing non-potable water could be provided until t = 60 min (pH between 6–9; Fe ≤ 5 mg L$^{-1}$ and Mn ≤ 0.5 mg L$^{-1}$) [45], and those for effluent launching could be provided until t ≈ 180 min (pH between 5–9; Fe ≤ 15 mg L$^{-1}$ and Mn ≤ 1 mg L$^{-1}$) [44].

Through the analysis of the Fe and Mn breakthrough curves (Fig. 6), the capacities of adsorption ($q$) of SS for Fe and Mn were determined. The capacities of adsorption ($q$, mg g$^{-1}$) were calculated using Eq. (12), where Q is the flow (mL min$^{-1}$), $C_0$ is the initial metal ion concentration (mg mL$^{-1}$) and w is the SS mass (g). In our case, $q$ resulted in 17.43 mg Fe per gram of SS and 3.87 mg Mn per gram of SS, values in consonance or higher than those found in the literature for other adsorbents [46–50]. This result is consonant with studies that evaluated the potential of chitin and chitosan (its deacetylated derivative) as biosorptive agents for the removal of industrial-relevant metal ions such as zinc, copper, chromium, cadmium, uranium, lead and others [51–54].

$$q = \frac{(t_e - \int_{t_b}^{t_e} f(t)dt)\, QC_0}{w} \quad (12)$$

The findings of this study demonstrate that shrimp shells can be used as a low-cost substrate to support the remediation of acidic and metal-laden waters. The obtained results indicate that this material can play a major role in the neutralization of acidic streams and the removal of metal contaminants. Additional tests are currently underway to evaluate the use of SS as an appropriate biomaterial in large-scale continuous-flow systems.

### 3.4. Chemical equilibrium modeling

pH dependent AMD remediation by sorption was investigated using chemical equilibrium modeling. AMD parameters, before and after continuous-flow column test (Table 8), were plotted and evaluated with Visual MINTEQ version 3.1. Input mass concentration for each component and Visual MINTEQ was run for predicting chemical equilibrium. The thermodynamic parameter was not modified in the database. The main production simulated with the software is shown in Table 9.

Meanwhile, the results on the percentage of ions indicated that 52.5% of Fe ion was identified as $FeSO_4$ (aq), 55.8% of Mn ion as $Mn^{2+}$ and 93.9% of S such as $SO_4^{2-}$. The results showed almost the same species percentage before and after treatment with pH increase close to neutrality. Thus, though AMD remediation is a pH dependent process, the modeling indicated the sorption mechanisms as a predominant

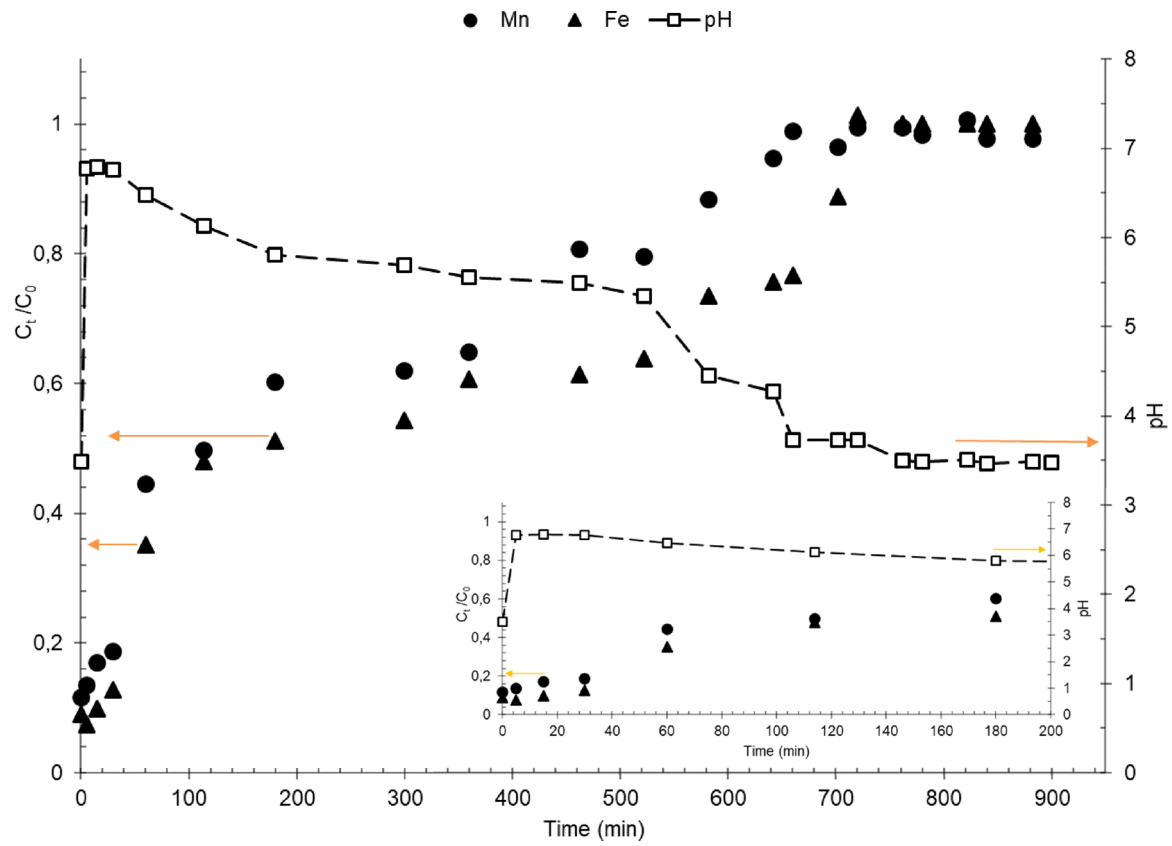


**Fig. 5.** Fe and Mn ion relative concentration ($C_t/C_0$) and pH variation versus contact time (min) in a continuous-flow fixed bed column test with an emphasis on the first 200 min of operation. Where $C_t$ and $C_0$ are the ion concentration (both in mg $L^{-1}$) at time t and initial time, respectively. The arrows indicate the respective ordinate axis of each parameter considered.

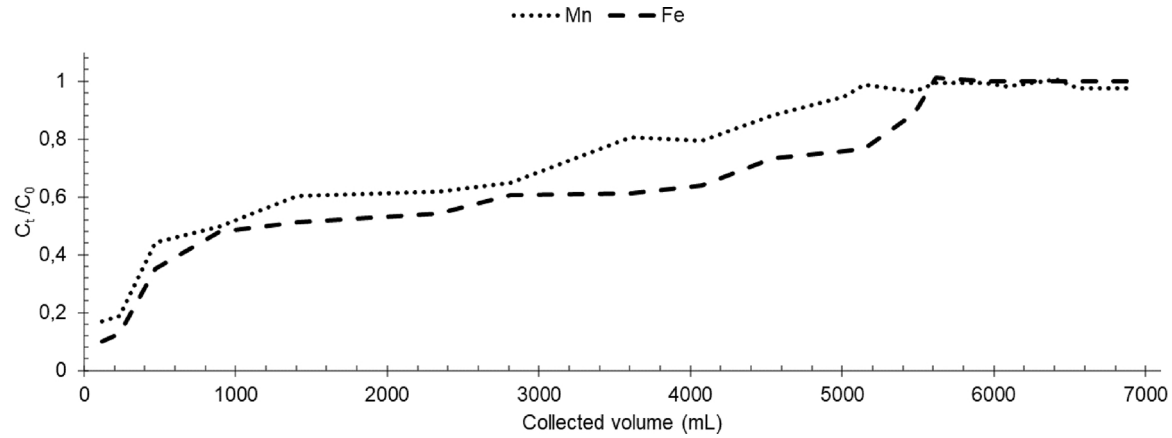


**Fig. 6.** Experimental breakthrough curves for the sorption of Fe and Mn ions onto SS fixed bed column. Where $C_t/C_0$ is the relative ion concentration (both in mg $L^{-1}$) and collected volume (mL) represents the total volume of AMD treated in the fixed bed column as a function of the operating time and the flow. AMD flow rate through the column was 7.8 $cm^3\,min^{-1}$. Effluent was collected at regular time intervals for residual metal ion estimation.

process in Fe and Mn remediation.

## 4. Conclusions

The Freundlich isotherm model was the best fitted for Fe and Mn ions removal, both in synthetic solutions and in natural AMD, indicating a physisorption mechanism. The model that best fitted the experimental data was determined by the correlation coefficients of the linearized equations and the study of the error non-linear statistical functions. The influence of the coexistence of metallic species in the sorption equilibrium processes was confirmed. The continuous-flow experiment showed that the effluent was according to Brazilian law parameters for water secondary non-potable reuse (until t = 60 min) and for no risk effluent launching (until t ≈ 180 min). The capacities of SS adsorption (q) resulted in 17.43 mg $g^{-1}$ and 3.87 mg $g^{-1}$. The suitability of the proposed treatment was confirmed, and the information is valuable for designing a low-cost remediation process for AMD. The chemical modeling indicated the sorption mechanism as a predominant process in the Fe and Mn remediation onto SS and confirmed the dependence of pH for AMD remediation. The findings of this study demonstrate that shrimp shells can be used as a low-cost substrate to support the remediation of acidic and metal-laden waters.

**Table 8**
AMD characterization before and after treatment with SS in descendent continuous-flow column. The values after treatment were calculated based on the results of operation of the fixed bed column until 60 min, where the adsorption mechanism was the main removal metal ion process.

| *Parameter* | Before treatment with SS Value | After treatment with SS |
|---|---|---|
| *pH* | 3.49 | 6.79 |
| | Concentration (mg $L^{-1}$) | |
| *Fe* | 83.24 | 3.1 |
| *Mn* | 14.70 | 2.9 |
| $SO_4^{2-}$ | 2300.00 | 2432.00 |

**Table 9**
Percentage distribution among dissolved and adsorbed species modeling with Visual MINTEQ 3.1.

| Component | Specie name | % of total concentration | |
|---|---|---|---|
| | | Before treatment | After treatment |
| $Fe^{2+}$ | $Fe^{2+}$ | 47.8 | 47.4 |
| | $FeSO_4$ (aq) | 52.2 | 52.5 |
| | $FeOH^+$ | – | 0.067 |
| $Mn^{2+}$ | $Mn^{+2}$ | 55.8 | 55.5 |
| | $MnSO_4$ (aq) | 44.2 | 44.5 |
| $SO_4^{2-}$ | $SO_4^{2-}$ | 93.9 | 95.7 |
| | $FeSO_4$ (aq) | 3.7 | 3.7 |
| | $MnSO_4$ (aq) | 0.56 | 0.57 |
| | $HSO_4^-$ | 1.7 | – |

## Declaration of Interest

None.

## Acknowledgements

The authors are grateful to the Department of Environmental Engineering at Federal University of Santa Catarina (UFSC) - Brazil for the technical support and National Council of Scientific and Technologic Development (CNPq, CT-Mineral 51/2013) for the financial support.

## Appendix A. Supplementary data

Supplementary material related to this article can be found, in the online version, at doi:https://doi.org/10.1016/j.jece.2018.11.032.

## References

[1] M.O. Álvarez, J.M.N. Líñán, A.M. Sarmiento, C.R. Cánovas, La contaminación minera de los ríos Tinto y Odiel, (2010) (Accessed 13 Septeber 2017), https://core.ac.uk/download/pdf/60665732.pdf.
[2] M.C.A. Trujillo, Recuperación de suelos de relaves mineros para convertirlos en áreas verdes en la planta piloto metalúrgica de *yauris-uncp*, Convicciones 2 (1) (2016) 36–43 (Accessed 28 November 2017), http://revistas.uncp.edu.pe/index.php/convicciones/article/download/192/188.
[3] T. Valente, J.A. Grande, M.L. de la Torre, P. Gomes, M. Santisteban, J. Borrego, M.S. Braga, Mineralogy and geochemistry of a clogged mining reservoir affected by historical acid mine drainage in an abandoned mining area, J. Geochem. Explor. 157 (2015) 66–76, https://doi.org/10.1016/j.gexplo.2015.05.016.
[4] W.H. Strosnider, F.S. Llanos, C.E. Marcillo, R.R. Callapa, R.W. Nairn, Impacto en afluentes del río Pilcomayo por contaminantes adicionales de drenaje ácido de minas desde cerro rico, Potosí-Bolivia, Av. Cienc. Ing. 5 (3) (2014) (Accessed 28 November 2017), http://www.redalyc.org/html/3236/323632128001/.
[5] J.W.N. Tempelhoff, M. Ginster, S. Motloung, C.M. Gouws, J.S. Strauss, The 2012 acid mine drainage (AMD) crisis in Carolina's municipal water supply, Afr. Hist. Rev. 46 (2) (2014) 77–107, https://doi.org/10.1080/17532523.2014.943978.
[6] N.Z. Alexandre, A.S.J. Krebs, Discussão da aplicação do método do IQI na avaliação da qualidade das águas da região carbonífera de Santa Catarina, Rev. Tecnol. Ambiente 2 (1996) 31–52.
[7] P.J. Borm, Toxicity and occupational health hazards of coal fly ash (CFA). A review of data and comparison to coal mine dust, Ann. Occup. Hyg. 41 (6) (1997) 659–676, https://doi.org/10.1093/annhyg/41.6.659.
[8] J.W. Owens, S.M. Swanson, D.A. Birkholz, Environmental monitoring of bleached Kraft pulp mill chlorophenolic compounds in a Northern Canadian river system, Chemosphere 29 (1) (1994) 89–109, https://doi.org/10.1016/0045-6535(94)90093-0.
[9] J.R.D. Amaral Filho, I.A.H. Schneider, I.A. de Brum, C.H. Sampaio, G. Miltzarek, C. Schneider, Characterization of a coal tailing deposit for integrated mine waste management in the Brazilian coal field of Santa Catarina, Rem: Rev. Esc. Minas 66 (3) (2013) 347–353, https://doi.org/10.1590/S0370-44672013000300012.
[10] P.G. Soares, Z.C. Castilhos, Recuperação de áreas degradadas pela mineração no Brasil. IV Jornada do Programa de Capacitação Interna – CETEM, (2015) http://mineralis.cetem.gov.br/bitstream/cetem/1802/1/5%20-%20Pablo_Soares_JPCI_2015%20impresso.pdf.
[11] V.T. Fávere, R. Laus, M.C.M. Laranjeira, A.O. Martins, R.C. Pedrosa, Use of chitosan microspheres as remedial material for acidity and iron (III) contents of coal mining wastewaters, Environ. Technol. 25 (8) (2004) 861–866, https://doi.org/10.1080/09593330.2004.9619378.
[12] P.C. Singer, W. Stumm, Acidic mine drainage: the rate-determining step, Science 167 (3921) (1970) 1121–1123, https://doi.org/10.1126/science.167.3921.1121.
[13] V.P. Evangelou, Y.L. Zhang, A review: pyrite oxidation mechanisms and acid mine drainage prevention, Crit. Rev. Environ. Sci. Technol. 25 (2) (1995) 141–199, https://doi.org/10.1080/10643389509388477.
[14] International Network for Acid Prevention (INAP), The Global Acid Rock Drainage (GARD) Guide, (2009).
[15] H. Cheng, Y. Hu, J. Luo, B. Xu, J. Zhao, Geochemical processes controlling fate and transport of arsenic in acid mine drainage (AMD) and natural systems, J. Hazard. Mater. 165 (1–3) (2009) 13–26, https://doi.org/10.1016/j.jhazmat.2008.10.070.
[16] D. Núñez-Gómez, A.A. de Almeida Alves, F.R. Lapolli, M.A. Lobo-Recio, Aplication of the statistical experimental design to optimize mine-impacted water (MIW) remediation using shrimp-shell, Chemosphere 167 (2017) 322–329, https://doi.org/10.1016/j.chemosphere.2016.09.094.
[17] D. Núñez-Gómez, M.E. Nagel-Hassemer, F.R. Lapolli, M.Á. Lobo-Recio, Potential of shrimp-shell residue in Natura for the remediation of mine impacted water (MIW), Polímeros 26 (SPE) (2016) 1–7, https://doi.org/10.1590/0104-1428.1757.
[18] S. Nikolov, M. Petrov, L. Lymperakis, M. Friák, C. Sachs, H.O. Fabritius, J. Neugebauer, Revealing the design principles of high-performance biological composites using ab initio and multiscale simulations: the example of lobster cuticle, Adv. Mater. 22 (4) (2010) 519–526, https://doi.org/10.1002/adma.200902019.
[19] SIRHESC – Sistema de informações de recursos hídricos do Estado de Santa Catarina, (2014) http://www.aguas.sc.gov.br/.
[20] D. Núñez-Gómez, F.R. Lapolli, M.E. Nagel-Hassemer, M.Á. Lobo-Recio, Optimization of Fe and Mn removal from coal acid mine drainage (AMD) with waste biomaterials: statistical modeling and kinetic study, Waste Biomass Valorization (2018) 1–15, https://doi.org/10.1007/s12649-018-0405-8.
[21] D. Núñez-Gómez, F.R. Lapolli, M.E. Nagel-Hassemer, M.Á. Lobo-Recio, Optimization of acid mine drainage remediation with central composite rotatable design model, Energy Procedia 136 (2017) 233–238, https://doi.org/10.1016/j.egypro.2017.10.248.
[22] K.W. Edgell, USEPA Method Study 35, SW Method 3005, Acid Digestion of Waters for Total Recoverable or Dissolved Metals for Analyses by Flame Atomic Absorption Spectroscopy, Environmental Monitoring Systems Laboratory, Office of Research and Development, U.S. Environmental Protection Agency, 1989, https://www.epa.gov/sites/production/files/2015-12/documents/3005a.pdf.
[23] American Public Health Association, American Water Works Association - APHA, Standard Methods for the Examination of Water and Wastewater, American public health association, 1989.
[24] E. Repo, L. Malinen, R. Koivula, R. Harjula, M. Sillanpää, Capture of Co (II) from its aqueous EDTA-chelate by DTPA-modified silica gel and chitosan, J. Hazard. Mater. 187 (1–3) (2011) 122–132, https://doi.org/10.1016/j.jhazmat.2010.12.113.
[25] T.M. Abdel-Fattah, M.E. Mahmoud, S.B. Ahmed, M.D. Huff, J.W. Lee, S. Kumar, Biochar from woody biomass for removing metal contaminants and carbon sequestration, J. Ind. Eng. Chem. 22 (2015) 103–109, https://doi.org/10.1016/j.jiec.2014.06.030.
[26] B. Batchelor, Leach models for contaminants immobilized by pH-dependent mechanisms, Environ. Sci. Technol. 32 (11) (1998) 1721–1726, https://doi.org/10.1021/es970747y.
[27] J.Y. Park, B. Batchelor, A multi-component numerical leach model coupled with a general chemical speciation code, Water Res. 36 (1) (2002) 156–166, https://doi.org/10.1016/S0043-1354(01)00207-X.
[28] K.Y. Foo, B.H. Hameed, Insights into the modeling of adsorption isotherm systems, Chem. Eng. J. 156 (1) (2010) 2–10, https://doi.org/10.1016/j.cej.2009.09.013.
[29] A. Azzam, A. Elatrash, N. Ghattas, The co-precipitation of manganese by iron (III) hydroxide, J. Radioanal. Nucl. Chem. 2 (3–4) (1969) 255–262, https://doi.org/10.1007/BF02513737.
[30] K.B. Krauskopf, Separation of manganese from iron in sedimentary processes, Geochim. Cosmochim. Acta 12 (1–2) (1957) 61–84, https://doi.org/10.1016/0016-7037(57)90018-2.
[31] M. Jain, V.K. Garg, K. Kadirvelu, M. Sillanpää, Adsorption of heavy metals from multi-metal aqueous solution by sunflower plant biomass-based carbons, Int. J. Environ. Sci. Technol. 13 (2) (2016) 493–500, https://doi.org/10.1007/s13762-015-0855-5.
[32] H. Teng, C.T. Hsieh, Influence of surface characteristics on liquid-phase adsorption of phenol by activated carbons prepared from bituminous coal, Ind. Eng. Chem. Res.

37 (9) (1998) 3618–3624, https://doi.org/10.1021/ie970796j.
[33] H.A. Aziz, M.N. Adlan, K.S. Ariffin, Heavy metals (Cd, Pb, Zn, Ni, Cu and Cr (III)) removal from water in Malaysia: post treatment by high quality limestone, Bioresour. Technol. 99 (6) (2008) 1578–1583, https://doi.org/10.1016/j.biortech.2007.04.007.
[34] J. Ćurko, M. Matošić, V. Crnek, V. Stulić, I. Mijatović, Adsorption characteristics of different adsorbents and iron (III) salt for removing as (V) from water, Food Technol. Biotechnol. 54 (2) (2016) 250 10.17113%2Fftb.54.02.16.4064.
[35] I. Langmuir, The constitution and fundamental properties of solids and liquids. Part I. Solids, J. Am. Chem. Soc. 38 (11) (1916) 2221–2295, https://doi.org/10.1021/ja02268a002.
[36] Ö. Gerçel, H.F. Gerçel, A.S. Koparal, Ü.B. Öğütveren, Removal of disperse dye from aqueous solution by novel adsorbent prepared from biomass plant material, J. Hazard. Mater. 160 (2–3) (2008) 668–674, https://doi.org/10.1016/j.jhazmat.2008.03.039.
[37] K. Vijayaraghavan, T.V.N. Padmesh, K. Palanivelu, M. Velan, Biosorption of nickel (II) ions onto Sargassum wightii: application of two-parameter and three-parameter isotherm models, J. Hazard. Mater. 133 (1–3) (2006) 304–308, https://doi.org/10.1016/j.jhazmat.2005.10.016.
[38] M.I. Tempkin, V. Pyzhev, Kinetics of ammonia synthesis on promoted iron catalyst, Acta Phys. Chim. USSR 12 (1) (1940) 327.
[39] M.J. Horsfall, A.I. Spiff, A.A. Abia, Studies on the influence of mercaptoacetic acid (MAA) modification of cassava (*manihot sculenta cranz*) waste biomass on the adsorption of Cu2 + and Cd2 + from aqueous solution, Bull. Korean Chem. Soc. 25 (7) (2004) 969–976, https://doi.org/10.5012/bkcs.2004.25.7.969.
[40] R.A.K. Rao, M.A. Khan, B.H. Jeon, Utilization of carbon derived from mustard oil cake (CMOC) for the removal of bivalent metal ions: effect of anionic surfactant on the removal and recovery, J. Hazard. Mater. 173 (1–3) (2010) 273–282, https://doi.org/10.1016/j.jhazmat.2009.08.080.
[41] J.C.Y. Ng, W.H. Cheung, G. McKay, Equilibrium studies for the sorption of lead from effluents using chitosan, Chemosphere 52 (6) (2003) 1021–1030, https://doi.org/10.1016/S0045-6535(03)00223-6.
[42] M.C. Ncibi, Applicability of some statistical tools to predict optimum adsorption isotherm after linear and non-linear regression analysis, J. Hazard. Mater. 153 (1-2) (2008) 207–212, https://doi.org/10.1016/j.jhazmat.2007.08.038.
[43] W.T. Tsai, H.C. Hsu, T.Y. Su, K.Y. Lin, C.M. Lin, Adsorption characteristics of bisphenol-A in aqueous solutions onto hydrophobic zeolite, J. Colloid Interface Sci. 299 (2) (2006) 513–519, https://doi.org/10.1016/j.jcis.2006.02.034.
[44] Brazil, National Environment Council – Resolução CONAMA 430/2011, Provisions the Conditions and Standards of Effluents and Complements and Changes Resolution 357 From March 17, 2005, issued by the National Environment Council (CONAMA), 2011, http://www.mma.gov.br/port/conama/res/res11/res43011.pdf.
[45] Brazil, National Environment Council - Resolução CONAMA 357/2005, Establishes Provisions for the Classification of Water Bodies as Well as Environmental Directives for their Framework, Establishes Conditions and Standards for Effluent Releases and Makes Other Provisions, (2005) http://www.mma.gov.br/port/conama/res/res05/res35705.pdf.
[46] M.A. Robinson-Lora, R.A. Brennan, Anaerobic precipitation of manganese and co-existing metals in mine impacted water treated with crab shell-associated minerals, Appl. Geochem. 26 (5) (2011) 853–862, https://doi.org/10.1016/j.apgeochem.2011.02.006.
[47] J.S. Webb, S. McGinness, H.M. Lappin-Scott, Metal removal by sulphate-reducing bacteria from natural and constructed wetlands, J. Appl. Microbiol. 84 (2) (1998) 240–248 (Accessed 16 November 2017), http://www.academia.edu/download/40533196/Metal_removal_by_sulfate_reducing_bacter20151201-20018-1uhs2sw.pdf.
[48] M.A. Willow, R.R. Cohen, pH, dissolved oxygen, and adsorption effects on metal removal in anaerobic bioreactors, J. Environ. Qual. 32 (4) (2003) 1212–1221, https://doi.org/10.2134/jeq2003.1212.
[49] J. Skousen, C.E. Zipper, A. Rose, P.F. Ziemkiewicz, R. Nairn, L.M. McDonald, R.L. Kleinmann, Review of passive systems for acid mine drainage treatment, Mine Water Environ. 36 (1) (2017) 133–153, https://doi.org/10.1007/s10230-016-0417-1.
[50] O. Gibert, J. De Pablo, J.L. Cortina, C. Ayora, Sorption studies of Zn (II) and Cu (II) onto vegetal compost used on reactive mixtures for in situ treatment of acid mine drainage, Water Res. 39 (13) (2005) 2827–2838, https://doi.org/10.1016/j.watres.2005.04.056.
[51] T.C. Yang, R.R. Zall, Absorption of metals by natural polymers generated from seafood processing wastes, Ind. Eng. Chem. Prod. Res. Dev. 23 (1) (1984) 168–172 https://10.1021/i300013a033.
[52] M.N.R. Kumar, A review of chitin and chitosan applications, React. Funct. Polym. 46 (1) (2000) 1–27, https://doi.org/10.1016/S1381-5148(00)00038-9.
[53] S.E. Bailey, T.J. Olin, R.M. Bricka, D.D. Adrian, A review of potentially low-cost sorbents for heavy metals, Water Res. 33 (11) (1999) 2469–2479, https://doi.org/10.1016/S0043-1354(98)00475-8.
[54] S. Babel, T.A. Kurniawan, Low-cost adsorbents for heavy metals uptake from contaminated water: a review, J. Hazard. Mater. 97 (1–3) (2003) 219–243, https://doi.org/10.1016/S0304-3894(02)00263-7.